Li and Shen *Earth, Planets and Space* (2015) 67:29
DOI 10.1186/s40623-015-0188-0

Earth, Planets and Space
a SpringerOpen Journal

FULL PAPER Open Access

Monthly GRACE detection of coseismic gravity change associated with 2011 Tohoku-Oki earthquake using northern gradient approach

Jin Li[1,2] and Wen-Bin Shen[1,3*]

Abstract

We demonstrate that the coseismic gravitational changes due to the 2011 $M_w = 9.0$ Tohoku-Oki earthquake are detectable by GRACE with only 1-month data after the earthquake, which is also supported by a simulation test using the seismic-signal-contained observations synthesized with the signals of a dislocation model prediction. The commonly used destriping to filter correlated errors in GRACE coefficients tends to distort the true coseismic signals in both amplitude and spatial pattern. In order to better retrieve coseismic gravitational signals, we apply a northern gravity gradient approach with the filter of spatial averaging and without destriping. The coseismic northern gravity gradient changes of Tohoku-Oki earthquake are extracted from the monthly data of April 2011, which reveal a positive-negative-positive spatial pattern and agree with the model prediction. The northern gradient approach provides an efficient means to detect coseismic signals and potentially constrain fault slip models with large-scale gravitational changes using limited time span of monthly GRACE solutions.

Keywords: Monthly GRACE solution; Coseismic gravity change; Northern gravity gradient; Dislocation model; Tohoku-Oki earthquake

Background

Coseismic gravity changes of very large earthquakes have been detected by Gravity Recovery and Climate Experiment (GRACE) since its launch in 2002, including the 2004 $M_w = 9.1$ Sumatra-Andaman earthquake (e.g., Han et al. 2006; Chen et al. 2007), 2010 $M_w = 8.8$ Maule (Central Chile) earthquake (e.g., Han et al. 2010; Heki and Matsuo 2010), 2011 $M_w = 9.0$ Tohoku-Oki earthquake (e.g., Matsuo and Heki 2011; Han et al. 2011; Wang et al. 2012a; Zhou et al. 2012; Cambiotti and Sabadini 2012, 2013; Dai et al. 2014), and the 2012 $M_w = 8.6$ Wharton basin earthquake off-Sumatra (Han et al. 2013). Attributing to the wide availability of various seismologic and geodetic observations for the Japan areas, the slips associated with 2011 Tohoku-Oki earthquake have been well constrained, using seismic wave data (e.g., Hayes 2011; Shao et al. 2011; Suzuki et al. 2012), land global positioning system (GPS) and seafloor bathymetry data (e.g., Chang and Chao 2011; Ito et al. 2011; Suito et al. 2011; Sato et al. 2011; Sleep 2012), InSAR data (e.g., Kobayashi et al. 2011), etc. As the second largest earthquake event during the GRACE mission, the Tohoku-Oki earthquake has provided good opportunities to verify the GRACE's sensitivity as well as its potential constraint to study huge earthquakes.

GRACE level 2 data released with monthly spherical harmonic (SH) coefficients are contaminated by north-south stripe errors, and the stripe errors are related with the correlated errors among the SH coefficients (Swenson and Wahr 2006). To suppress the correlated errors, a high-pass filter is usually designed by fitting the coefficients with polynomials, which is considered as destriping. Chen et al. (2007) and Heki and Matsuo (2010) used a filter including destriping first and then spatial averaging to reduce noises and retrieve seismic signals associated with large earthquakes. Several other previous studies also employed destriping to extract the coseismic gravitational changes due to 2011 Tohoku-Oki earthquake (e.g., Matsuo and Heki 2011; Zhou et al. 2012). Nevertheless, destriping would distort and reduce real signals while suppressing

* Correspondence: wbshen@sgg.whu.edu.cn
[1]Department of Geophysics, School of Geodesy and Geomatics, Wuhan University, Wuhan 430079, China
[3]State Key Laboratory of Information Engineering in Surveying, Mapping and Remote Sensing, Wuhan University, Wuhan 430079, China
Full list of author information is available at the end of the article

stripes. Li and Shen (2011) found that the horizontal components of gravity gradient changes exhibit positive-negative-positive features due to the mass variations of a large thrusting earthquake and recommended a northern (latitude-direction) gravity gradient approach to detect the coseismic effects more efficiently due to the anisotropic sensitivity of GRACE observations. Later, Wang et al. (2012b) demonstrated the potential of gravity gradient approach in a more general sense. So far, GRACE observations have been applied to constrain fault slip models with large-scale gravity changes, but mostly from the direct use of level 1B (range and range-rate) data (e.g., Han et al. 2010, 2011, 2013). For the potential application of GRACE level 2 monthly solutions to constrain fault slips (which would be much more convenient by the simple processing of SH coefficients, if possible), it is essential to suppress stripe errors and retrieve true signals as much as possible for the observations.

In order to demonstrate the advantage of the northern gravity gradient approach in reducing stripe errors and extracting coseismic signals, we design a synthetic test based on the co- and postseismic gravity changes of the Tohoku-Oki earthquake predicted by a dislocation model. We obtain the seismic-signal-contained synthetic GRACE observations by adding the model-predicted gravity changes to real GRACE data. Then we retrieve the gravity changes and northern gravity gradient changes from the synthetic observations, in order to find out whether and how much the coseismic signature of the earthquake could be detected. Furthermore, we verify the synthetic results by retrieving the Tohoku-Oki earthquake's coseismic signals with the real GRACE data of April 2011. Results demonstrate the detecting sensitivity using the northern gravity gradient changes even with very limited time span (e.g. only 1 month after the earthquake) of GRACE level 2 monthly data.

Methods

Synthetic test

We calculate the coseismic land-surface deformations a well as the co- and postseismic gravity changes based on a layered viscoelastic gravitational half-space dislocation model, using the PSGRN/PSCMP code provided by Wang et al. (2006). The Earth model is divided into five layers, the upper four of which are in the elastic crust and the lower half-space part (i.e., the upper mantle) is considered as a Maxwell body (see Table 1). The fault slip model is from GPS and waveform inversion by Wei et al. (2011).

Based on the dislocation model we predict the coseismic deformations at 847 GPS sites and compare them with GPS displacement observations. The GPS displacements of the 847 points are from the preliminary solution (version 1.0) provided by the ARIA team at JPL and Caltech. These 847 points are picked up from the total 1,232 sites with the epicentral distances less than 1,000 km, among which 474 points locate within 600 km epicentral distance (Figure 1a,b), while the other 373 points are within epicentral distances from 600 to 1,000 km (Figure 1c,d). Figure 1a shows the predicted and observed horizontal displacements at the 474 GPS sites with magenta and black arrows, respectively, and Figure 1b shows the corresponding vertical displacements with a different arrow scale. The predicted and observed coseismic displacements agree well in both amplitude and direction for most of the GPS sites. Since the fault slip model inversion of Wei et al. (2011) used the same GPS data, the agreement of the model-predicted and the GPS-observed displacements here would validate the Earth model used in this study.

Table 1 The five-layer half-space Earth model used in the prediction of co- and postseismic gravity changes

Depth (km)	Density (ρ) (10^3 kg m^{-3})	V_P (km s^{-1})	V_S (km s^{-1})	Viscosity (η) (10^{19} Pa s)	Material type
0-1	2.10	2.10	1.00	∞	Elastic
1-8	2.70	6.00	3.40	∞	Elastic
8-15	2.90	6.60	3.70	∞	Elastic
15-22	3.05	7.20	4.00	∞	Elastic
22-∞	3.40	8.20	4.70	0.93	Maxwell body

The layer depths, densities, and seismic velocities are extracted from the CRUST2.0 global tomography model (Bassin et al. 2000), and the viscosity of the upper mantle is quoted from Sato et al. (1981) and Suito and Hirahara (1999).

As the PSGRN/PSCMP program computes the gravity changes on the deformed land surface, we add back the free-air corrections (obtained according to the vertical surface displacements) to the calculated values in order to recover the gravity changes at the space-fixed points (Sun et al. 2009). Moreover, a Bouguer layer correction of seawater (also calculated by the vertical surface displacements) is compensated to the gravity changes in oceanic areas (Heki and Matsuo 2010). We disassemble the model-predicted gravity changes into SH coefficients to degree 60, remove the 0 and 1 degree terms, and then average them with 300 km isotropic Gaussian smoothing, in order to obtain a comparable spatial resolution as GRACE. After spatial averaging, the predicted coseismic gravity changes range from −11.7 to +5.6 μGal (note that 1 μGal equals 1×10^{-8} m s^{-2}) as depicted in Figure 2a. The negative-positive pattern of coseismic gravity changes is associated with not only the uplift-subsidence deformation caused by elastic rebound but also the density decrease due to crustal dilatation as discussed by Han et al. (2006). We also predict the postseismic gravity changes of 24 months in the 2 years after the earthquake. The postseismic gravity changes principally show slow linear positive trends with a maximum rate of 0.40 μGal year^{-1}

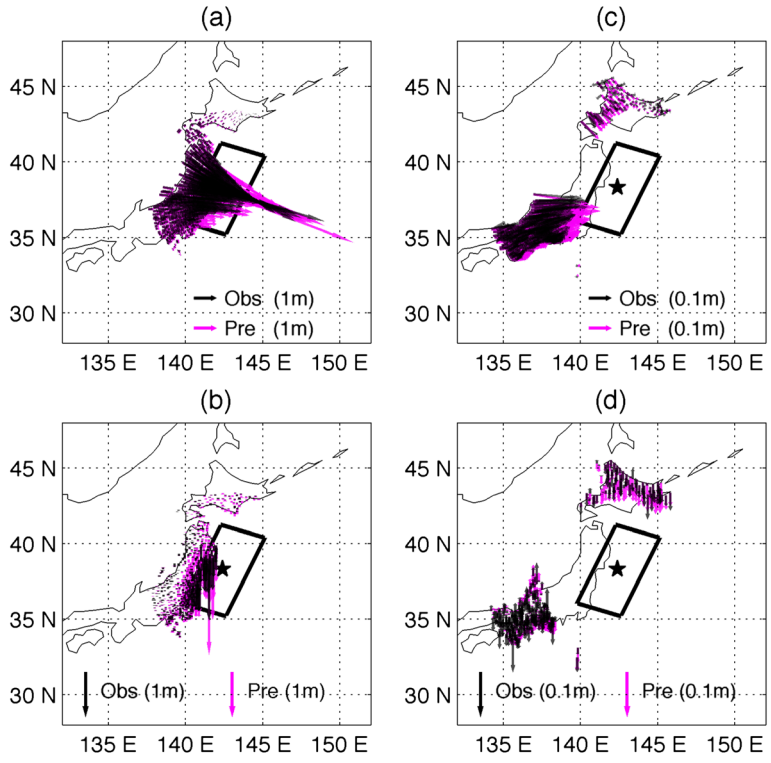

Figure 1 The observed (black arrows) and predicted (magenta arrows) coseismic displacements at the 847 GPS sites. (a) and **(b)** Horizontal and vertical displacements, respectively, at 474 sites within 600 km epicentral distance. **(c)** and **(d)** Horizontal and vertical displacements, respectively, at the other 373 sites with epicentral distances from 600 to 1,000 km. The black rectangle denotes the boundary projection of the fault plane and the black pentagram indicates the epicenter (the same in subsequent figures).

surrounding the epicenter (Figure 2b). In the computation, we pick up a region ranging from 28°N to 48°N in latitude and 132°E to 152°E in longitude as the region of interest. The epicenter (38.1°N, 142.8°E) locates at the center of the region. The cell size of the grid is set to 0.2° × 0.2°.

The monthly GRACE gravity solutions used in the synthetic test are level 2 (RL05) products from the University of Texas Center for Space Research (UTCSR), including 49 monthly data sets from January 2007 to February 2011 (with the data of January 2011 absent due to observing problems of the GRACE satellites). Each monthly data set consists of the SH coefficients with degree and order to 60. We replace the GRACE C_{20} coefficients with SLR estimates (Cheng and Tapley 2004; Cheng et al. 2013). We also note that the 0 and 1 degree terms are not included in the computation, as the GRACE monthly solutions do not recover the degree 0 and 1 SH coefficients for the Earth's time-variable gravitational field.

In the synthetic test, we assume that an identical earthquake as the Tohoku-Oki event occurred in March 2009 at the same place in the Japan Trench. We disassemble the model-predicted co- and postseismic gravity changes into SH coefficients to degree 60, omit the 0 and 1 degree terms, and add the predicted SH coefficients to the monthly GRACE data. The converted model SH-coefficient data sets cover the period from March 2009 to February 2011, with that of January 2011 excluded due to the absence of GRACE data for this month. By the above synthesizing, 2 years of seismic-signal-contained GRACE observations after the synthetic earthquake are available for the synthetic test.

We apply a modified stacking approach based on that from Chen et al. (2007) to retrieve the coseismic signals in the synthetic monthly GRACE observations. While Chen et al. (2007) directly stack the monthly data sets of a time span to obtain the mean field before and after the earthquake, here we remove the seasonal variations and also the linear trends (before and after the earthquake, respectively) by time series fitting before the stacking. The fitting in advance to the stacking would evidently reduce the impact of linear trends preceding and following the earthquake, which could contaminate the coseismic jumps if retrieved by direct stacking. It should be noted that the seasonal variations would also affect the coseismic signal retrieval when the time span is less than 1 year for the direct stacking approach. To implement the modified stacking approach, first we filter the GRACE coefficients with destriping and Gaussian smoothing and calculate the

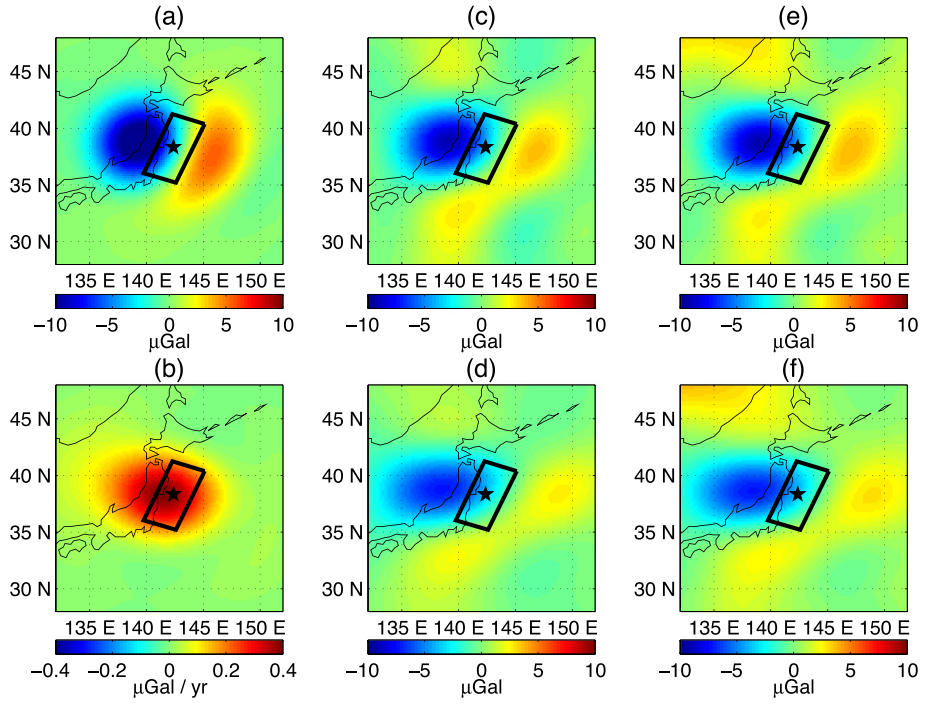

Figure 2 Model-predicted and synthetic-data-retrieved seismic gravity changes due to 2011 Tohoku-Oki earthquake. (a) Model prediction of coseismic gravity changes, with 300 km Gaussian smoothing only. **(b)** Trend term obtained by fitting gridded time series of model-predicted postseismic gravity changes of 24 months in 2 years after the earthquake, with 300 km Gaussian smoothing. **(c)** Model prediction of the coseismic gravity changes same as **(a)** but with P3M6 destriping and 300 km Gaussian smoothing. **(d)** Model prediction of coseismic gravity changes with Duan09 destriping and 300 km Gaussian smoothing. **(e)** Gravity changes between the mean of 2 years before and after the earthquake, computed from the synthetic monthly GRACE observations (with seasonal and trend terms removed by time series fitting), with a filter of P3M6 destriping and 300 km Gaussian smoothing. **(f)** Gravity changes same as **(e)** but with a different filter, Duan09 destriping, and 300 km Gaussian smoothing. Note that 1 μGal equals 1×10^{-8} m s^{-2} in gravity change.

gravity changes at the grid points in the region of interest. Then we remove the seasonal variations and linear trends by the time series fitting, which consists of two linear trend terms before and after the earthquake, seasonal (including annual and semiannual) terms, and a piecewise step term preceding and following the earthquake.

For the destriping processing, we employ two approaches, one of which is the P3M6 destriping from Chen et al. (2007) and the other is the method provided by Duan et al. (2009) (referred as Duan09 destriping hereinafter). For the sake of comparing the retrieved coseismic signals (from synthetic observations) with model prediction under same data processing, we provide the model-predicted gravity changes after destriping plus 300 km Gaussian smoothing in Figure 2c,d, for P3M6 and Duan09 destriping approaches, respectively. Compared with the '−11.7 to +5.6 μGal' results without destriping (Figure 2a), the peak-to-peak range of model gravity changes is evidently reduced, to '−9.1 to +3.6 μGal' (Figure 2c) and '−7.3 to +2.6 μGal' (Figure 2d), respectively. Moreover, the spatial pattern after destriping is distorted, namely, extruded wider in the east-west direction. This reveals the obvious impact of destriping filter on coseismic gravity changes, both in amplitude and spatial pattern. The Duan09 destriping appears to reduce the amplitude and distorts the spatial pattern even more, probably due to its stronger filter to SH coefficients.

From the 4-year synthetic GRACE observations, we obtain the differences between the mean over 2 years before (from April 2007 to February 2009) and after (from April 2009 to February 2011) the synthetic earthquake, which are considered as the coseismic gravity changes retrieved by stacking approach. The gravity changes are shown in Figure 2e,f, representing the results by the filter of P3M6 destriping plus 300 km Gaussian smoothing and by that of Duan09 destriping plus 300 km Gaussian smoothing, respectively. For the land area at the northwestern corner of the region of interest, the extracted gravity changes exhibit positive anomalies (see both Figure 2e,f), which are possibly related with the unfitted inter-annual hydrological effect as the area is quite far away from the epicenter. For the areas surrounding the epicenter, the gravity changes predominantly show negative-positive feature that is consistent with the model prediction. The peak-to-peak ranges are '−9.2 to +3.7 μGal' and '−7.3 to +3.5 μGal' for the results in Figure 2e,f,

respectively, agreeing well with the model-predicted coseismic gravity changes with corresponding filters in Figure 2c,d. The spatial patterns are also consistent between the retrieved and model-predicted gravity changes. Nevertheless, neither result in Figure 2c or 2d is the 'true signal' for the coseismic gravity changes with 300 km spatial resolution, as they are both reduced and distorted by the destriping filter. It should be noted that the destriping filter is dedicated to remove or reduce GRACE stripe errors, which means ideally it should not affect the true signature. But practically, it inevitably introduces artificial impact on the signals when applied to the model-predicted coseismic gravity changes. Thus, the true signal (under 300 km resolution) should be the gravity changes without destriping, as shown in Figure 2a. According to the peak-to-peak range and spatial pattern of true coseismic gravity changes (under 300 km resolution, see Figure 2a), the retrieved signals in Figure 2c,d evidently deviate from the truth, indicating that the destriping could lead to obvious effect of reduction and distortion for coseismic gravity changes.

We also calculate the coseismic northern gravity gradient changes in the region of interest, for both the model prediction and synthetic data retrieval. The northern gravity gradient changes are evaluated from the derivative of the associate Legendre function according to the spherical harmonic expansion of Earth's gravity field (e.g., Li and Shen 2011), based on the model and GRACE-synthetic SH coefficients, respectively. After spatial smoothing, the model-predicted northern gravity gradient changes are shown in Figure 3a,b,c, with the filters of 300 km Gaussian smoothing only, P3M6 destriping plus 300 km Gaussian smoothing, and Duan09 destriping plus 300 km Gaussian smoothing, respectively. Whichever filter is used, the model prediction shows dominant positive-negative-positive pattern. The peak-to-peak ranges reflect slight differences, as '+2.6 to -2.8 to +1.2' × 10^{-13} s^{-2}, '+2.5 to -2.7 to +1.1' × 10^{-13} s^{-2} and '+2.0 to -2.3 to +0.8' × 10^{-13} s^{-2} for Figure 3a,b,c, respectively. Again, the Duan09 destriping shows more coseismic signal reduction and distortion than the P3M6 destriping does. The coseismic northern gravity gradient changes retrieved from synthetic observations range from '+2.6 to -2.8 to +1.0' × 10^{-13} s^{-2} and '+2.2 to -2.4 to +0.8' × 10^{-13} s^{-2}, for the 'P3M6 destriping plus 300 km Gaussian smoothing' and 'Duan09 destriping plus 300 km Gaussian smoothing' filters, respectively (see Figure 3d,e). The retrieved northern gradient signals agree well with their

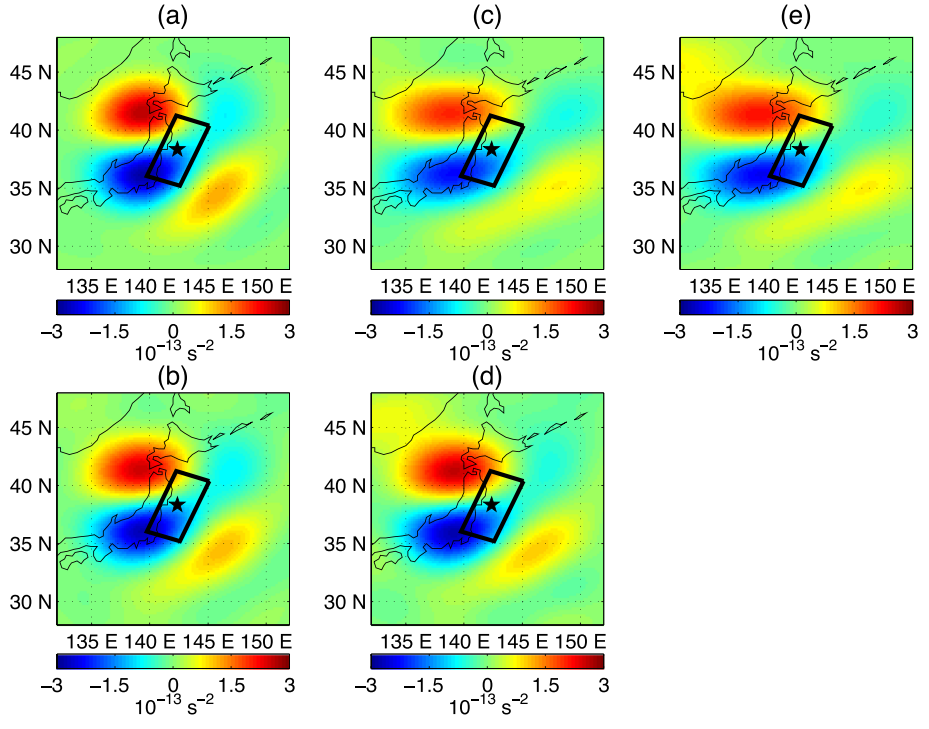

Figure 3 Model-predicted and synthetic-data-retrieved northern (latitude-direction) component of coseismic gravity gradient changes due to 2011 Tohoku-Oki earthquake. (a) Model prediction with 300 km Gaussian smoothing only. **(b)** Model prediction with P3M6 destriping and 300 km Gaussian smoothing. **(c)** Model prediction with Duan09 destriping and 300 km Gaussian smoothing. **(d)** Northern gravity gradient changes between the mean of 2 years before and after the earthquake, computed from the synthetic monthly GRACE observations (with seasonal and trend terms removed by time series fitting), with P3M6 destriping and 300 km Gaussian smoothing. **(e)** The retrieved northern gravity gradient changes same as **(d)** but with Duan09 destriping and 300 km Gaussian smoothing.

corresponding model results. In addition, the retrieved northern gradient changes generally show better agreement with the 'true gradient signal' (in Figure 3a), when compared with those for the retrieved gravity changes in Figure 2. This might be due to that the northern (latitude-direction) gradient would highlight the east-west pattern and suppress the north-south feature in the spatial feature of the signals, while the destriping filter is designed to reduce the north-south pattern stripes. Even though the agreement seems better, it should be noted that the retrieved gradient changes still exhibit discrepancies with the truth in both amplitude and spatial pattern. Therefore, one should keep in mind that the destriping filter would not only suppress errors but also reduce and distort true signals.

In order to keep away from the influence of destriping, we further implement the synthetic test with 300 km Gaussian smoothing only (without destriping) for both gravity-change and northern-gradient-change results. We calculate the gravity and northern gravity gradient changes between the mean of 2 years before and after the synthetic earthquake, from the synthetic monthly GRACE observations (with seasonal and trend terms removed by time series fitting). Figure 4a,b shows the gravity changes for the near field and global field, respectively. The global distribution is provided here to show the north-south stripes in a global-field viewpoint, which may display the stripes more clearly and visually. The global field in Figure 4b reveals that the stripes are a bit heavy because destriping is not applied to filter the correlated errors. For the near field in Figure 4a, the extracted coseismic gravity changes from −12.0 to +6.6 μGal agree not bad with the model prediction in Figure 2a, and the distribution is not evidently distorted (e.g., extruded wider) either. But it can be easily noted that the positive-gravity lobe stretches further to the north (compared with model prediction), which is probably due to the contamination of unfiltered stripe errors.

Figure 4c,d depicts the northern gravity gradient changes with 300 km Gaussian smoothing only (without destriping) for the near field and global field, respectively. As a result of the suppressing effect of the northern gravity

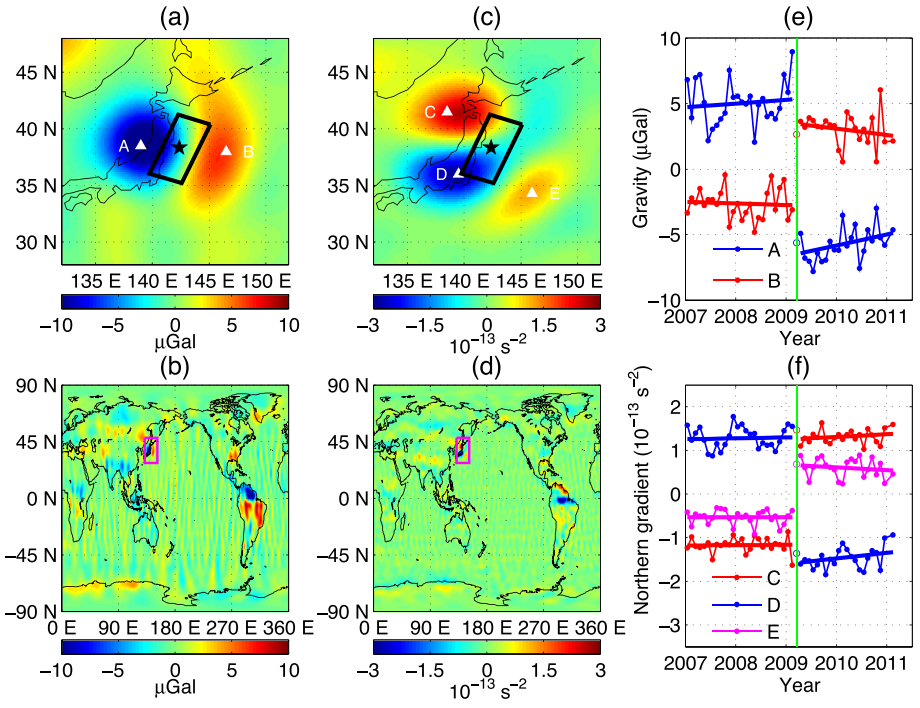

Figure 4 Gravity changes and northern gravity gradient changes with the mean of 2 years' synthetic data. The changes are between the mean of 2 years before and after the earthquake, computed from the synthetic monthly GRACE observations (with seasonal and trend terms removed by time series fitting), with 300 km Gaussian smoothing only (without destriping). **(a)** Near-field gravity changes. **(b)** Global gravity changes with cell size of 1° × 1°, in which the black rectangle denotes the region in **(a)**. **(c)** Near-field northern gravity gradient changes. **(d)** Global northern gravity gradient changes. **(e)** Time series of the synthetic monthly GRACE gravity values at points A (38.5°N, 139.0°E) and B (38.0°N, 146.5°E) marked as white triangles in **(a)**, from January 2007 to February 2011. **(f)** Time series of the synthetic monthly GRACE gravity gradient values at points C (41.5°N, 138.5°E), D (36.0°N, 139.5°E), and E (34.3°N, 146.0°E) marked as white triangles in **(c)**. The time series are fitted by two linear terms before and after the earthquake, the annual and semiannual periodic terms, and a coseismic step term. The linear trends before and after the earthquake as well as the coseismic jumps are shown with the solid lines. The vertical green line represents the occurrence month of the synthetic earthquake (i.e., March 2009). The magenta rectangles in **(b)** and **(d)** denote the region of the near field in **(a)** and **(c)**.

gradient changes on the north-south stripes, the signals in Figure 4d are less contaminated by stripes than those in Figure 4b. Since GRACE observations are of anisotropic sensitivity due to the along-orbit measurements of the two near-polar-orbit satellites, the signal-to-noise ratio (SNR) in the longitudinal direction should be higher (Li and Shen 2011). The positive-negative-positive gradient changes in the near field of Figure 4c range from '+2.6 to −2.9 to +1.2' $\times 10^{-13}$ s^{-2} and coincide quite well with the 'true signal' as shown in Figure 3a for both amplitude and spatial pattern. Therefore, Figure 4c indicates a better detection of the coseismic gravitational associated with the earthquake, where the retrieved signals are less contaminated by stripes (compared with that in Figure 4a), attributing to the suppressing effect of northern gradient approach on GRACE stripe errors even though destriping is not applied here.

Figure 4e,f denotes the time series from January 2007 to February 2011 of the synthetic GRACE observations at some picked-up points marked as white triangles in Figure 4a,c, with the filter of 300 km Gaussian smoothing only (without destriping) to the monthly synthetic data. The time series show that the amplitude of the jumps at the time of earthquake is larger than that of the other variations during the period of 4 years, indicating that the coseismic gravitational changes of the earthquake are within the observing capability of GRACE. We fit the time series with seasonal (annual and semiannual) terms, linear trend terms before and after the synthetic earthquake (respectively), and a coseismic jump term. Then we extract the linear trends before and after the earthquake and also the coseismic jumps (see the solid-step lines in Figure 4e,f). The coseismic gravity and gravity-gradient jumps are well retrieved by the fitting of time series when compared with the model prediction. Nevertheless, it could be noted that there are some irregular peaks in the time series of gravity changes in Figure 4e possibly due to the unfiltered stripe errors, while the time series of northern gravity gradient changes in Figure 4f show relatively smaller irregular peaks, again demonstrating the suppressing ability of the northern gradient changes.

In order to find out whether the coseismic gravitational signals could be detected by a shorter time span of data, we calculate the gravity and gravity gradient changes with only 1-month observation after the synthetic earthquake (i.e., April 2009) for the test. Gravity changes and northern gravity gradient changes are obtained from the field of April 2009 with respect to the mean field of 2 years before the synthetic earthquake. It should be noted that the seasonal and trend terms are removed first by time series fitting from the synthetic observations. The near-field changes (see top panels) and global-field changes (see bottom panels) are shown in Figure 5. The gravity changes and northern gravity gradient changes with 300 km Gaussian smoothing only (without destriping) are depicted in Figure 5a,b and Figure 5c,d, respectively. Figure 5e,f shows the gravity changes with the filter of P3M6 destriping and 300 km smoothing. Even though the negative-positive pattern in gravity changes and the positive-negative-positive feature in northern gradient changes are still obviously detected, the signals retrieved from the 1-month data set are more contaminated by stripes than those from the 2-year data (see Figure 4a,b,c,d) due to the absence of stacking to suppress stripe errors. Again the northern gravity gradient changes show less stripes (compare Figure 5d with Figure 5b) and a better detection than the gravity changes (compare the retrieved changes with the corresponding true signals in Figures 2a and 3a). When the P3M6 destriping is applied to filter the data, the extracted gravity changes are reduced in amplitude and also distorted in spatial pattern (compare Figure 5e with Figure 2a) even though the stripes decrease to some extent (see Figure 5f).

Based on synthetic tests, we could take advantage of the prior knowledge for the true signal; thus, we are able to assess the efficiency and reliability of the GRACE filter in retrieving coseismic gravity changes. According to the results by synthetic test, we find that the destriping filter tends to evidently reduce the amplitude and distort the spatial pattern of the true coseismic signals. Nevertheless, the northern gravity gradient approach provides a good means to suppress stripe errors and extract coseismic signals from GRACE observations. The positive-negative-positive pattern in northern gradient changes could better capture the coseismic signals than the negative-positive pattern from gravity changes. Therefore, to retrieve the coseismic variations using monthly GRACE solutions, we suggest using the northern gradient approach and employing the spatial averaging (e.g., Gaussian smoothing) only without destriping. This recommended gradient approach especially applies for the case of detecting coseismic gravitational changes with a time span of limited length (e.g., a few months or even only 1 month after the earthquake).

Results

One-month GRACE data detection

Here we provide the results of detecting the coseismic changes due to the Tohoku-Oki earthquake with only 1 month of GRACE solutions (April 2011), as shown in Figure 6. We obtain the gravity and northern gravity gradient changes from the field of April 2009 with respect to the mean field of 4 years (from January 2007 to December 2010) before the earthquake. It should be noted that the seasonal (annual and semiannual) terms as well as the trend term before the earthquake are removed by time series fitting from the 51 months of

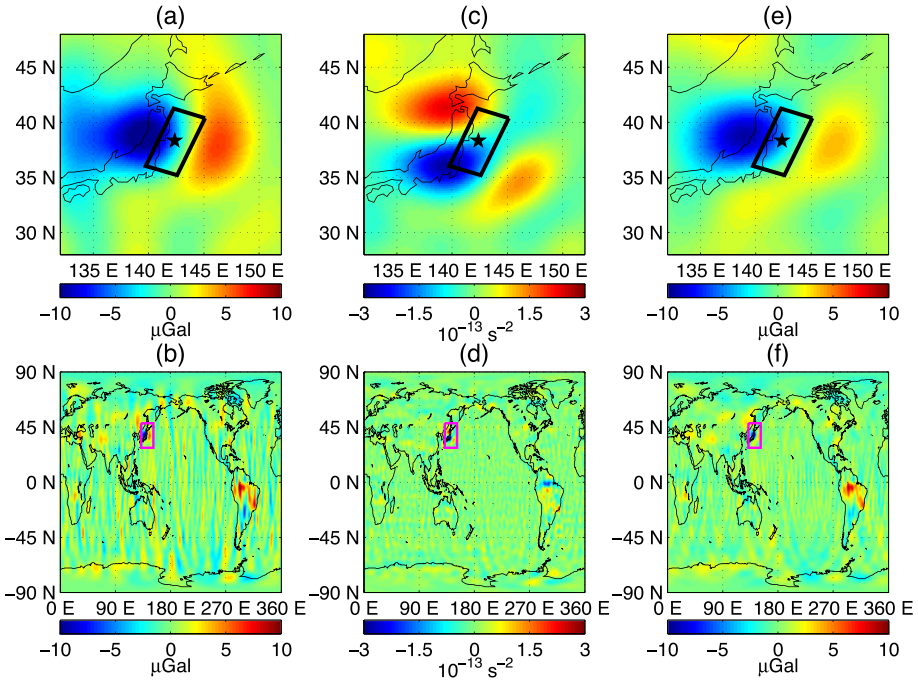

Figure 5 Gravity changes and northern gravity gradient changes from the April 2009 synthetic data. The changes occur 1 month after the synthetic earthquake with respect to the mean field of 2 years before the synthetic earthquake, computed by the synthetic monthly GRACE observations (with seasonal and trend terms removed by time series fitting). **(a)** Near-field gravity changes, with 300 km Gaussian smoothing only (without destriping). **(b)** Global gravity changes, in which the black rectangle denotes the region in **(a)**. **(c)** Near-field northern gravity gradient changes, with 300 km Gaussian smoothing only. **(d)** Global northern gravity gradient changes. **(e)** Near-field gravity changes, with P3M6 destriping and 300 km Gaussian smoothing. **(f)** Global gravity changes, with the filter same as applied in **(e)**. The magenta rectangles in **(b)**, **(d)**, and **(f)** denote the region of the near field in **(a)**, **(c)**, and **(e)**.

GRACE observations (note the data set for January 2011 is absent in level 2 data release). We do not include the trend term after the earthquake for the time series fitting as done in the synthetic test, because there is only 1-month data set after the earthquake. Figure 6a depicts the gravity changes with 300 km Gaussian smoothing only, and Figure 6b,c shows the gravity changes with the filters of 'P3M6 destriping plus 300 km Gaussian smoothing' and 'Duan09 destriping plus 300 km smoothing', respectively. The peak-to-peak ranges of the gravity changes are −8.7 to +3.3 μGal, −7.9 to +2.2 μGal, and −7.0 to +1.5 μGal, for Figure 6a,b,c, respectively. For the results in Figure 6a, the positive pattern of gravity changes probably shows the feature of the GRACE stripes as it stretches a bit further to both north and south and locates kind of farther eastward away from the fault plane. We also note that there is a stripe-feature lobe of negative gravity changes at the easternmost edge of the region (see the blue lobe at longitudes more than 150°E in Figure 6a), which possibly implies that the results with 300 km Gaussian smoothing only are obviously contaminated by stripe errors. After the destriping filters are applied, the results appear cleaner (as shown in Figure 6b,c), but the spatial pattern of negative-positive changes is distorted (stretched wider in the east-west direction) and the amplitude is reduced. Particularly, the gravity-increase lobes are almost invisible for the oceanic areas on the east of the fault plane, in both Figure 6b,c. This demonstrates the evident artificial impact of destriping filter on the coseismic gravity-change retrieval. Therefore, it could be inferred that the gravity-change approach with the filter of destriping plus spatial averaging may not work well for detecting coseismic signals with only 1-month GRACE data set, as the SNR for the observation is relatively weak for this case.

In consideration of the northern gravity gradient approach recommended by the synthetic test, we provide the northern gradient changes in Figure 6d,e, with the filters of '300 km Gaussian smoothing only' and 'P3M6 destriping plus 300 km Gaussian smoothing', respectively. We retrieve obvious positive-negative-positive patterns of gradient changes for both results in Figure 6d,e, with peak-to-peak ranges of '+1.7 to −2.3 to +0.8' × 10^{-13} s^{-2} and '+1.8 to −2.2 to +0.8' × 10^{-13} s^{-2}, respectively. The positive-negative-positive spatial pattern agrees well with the model prediction for northern gravity gradient changes in Figure 3a. We also provide the northern gravity gradient changes from GRACE data set 1 month before the earthquake (February 2011), which are supposed

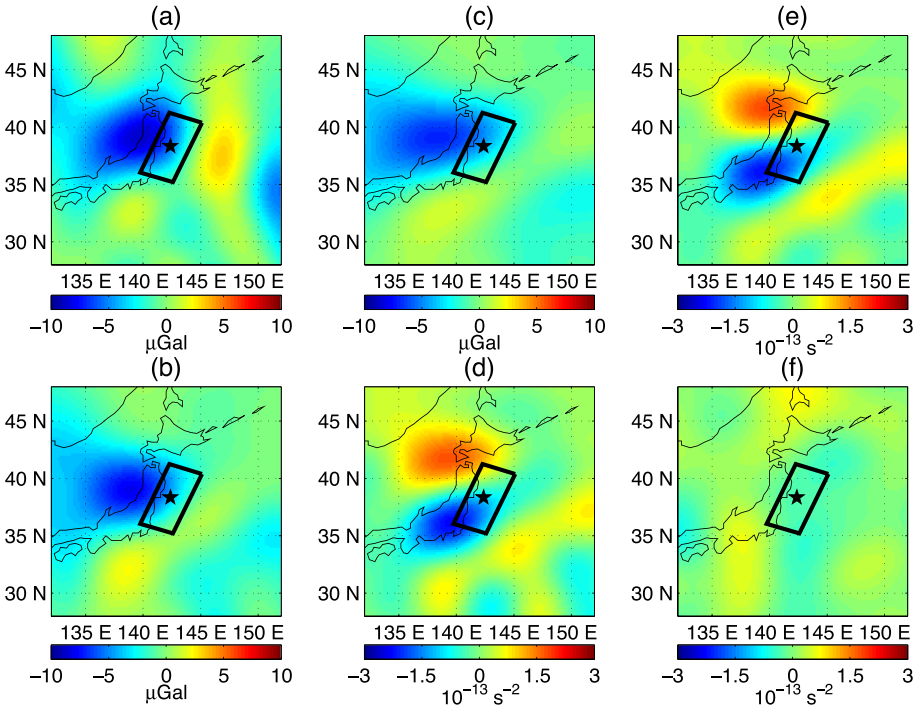

Figure 6 Real data detection of coseismic gravity field changes. The gravity field changes associated with Tohoku-Oki earthquake are obtained using 1 month GRACE solution of April 2011. **(a)** Gravity changes of April 2011 with respect to the mean of 4 years from January 2007 to December 2010 (as the background field), with 300 km Gaussian smoothing and without destriping. **(b)** Gravity changes same as **(a)** but with P3M6 destriping and 300 km Gaussian smoothing. **(c)** Gravity changes same as **(a)** but with Duan09 destriping and 300 km Gaussian smoothing. **(d)** Northern gravity gradient changes of April 2011 with respect to the 4-year mean field, with 300 km Gaussian smoothing and without destriping. **(e)** Northern gravity gradient changes same as **(d)** but with P3M6 destriping and 300 km Gaussian smoothing. **(f)** Northern gravity gradient changes of February 2011 with respect to the 4-year mean field, with 300 km Gaussian smoothing and without destriping.

not to contain the coseismic signals. The results with 300 km Gaussian smoothing only are shown in Figure 6f. The gradient changes of February 2011 range relatively smaller than those of April 2011, from −0.7 to +0.7 × 10^{-13} s^{-2}, and do not show any obvious positive-negative-positive pattern around the fault plane. The peak-to-peak range of gradient changes for the February 2011 field probably imply the variation level from the unfiltered GRACE stripe errors as well as other land and oceanic mass-change effects in the region, which is significantly under the positive-negative-positive amplitude of signals detected from the April 2011 field. This demonstrates that the coseismic northern gravity-gradient changes are well detectable using only 1-month GRACE solution after the 2011 Tohoku-Oki earthquake and also verifies the conclusions of the synthetic test.

Despite the good agreement in positive-negative-positive spatial pattern between retrieved and model-predicted northern gravity gradient changes, the amplitude of retrieved results is smaller than that of the model prediction (compare Figure 6d,e with Figure 3a,b, respectively). The reduction in amplitude for the signal retrieval possibly attributes to the influence of residual stripes in the monthly GRACE data, as only 1-month data set is used for the signal extraction and thus the SNR is relatively weaker compared with that from series of data sets. One should also keep in mind that the northern gradient approach could only suppress (or reduce) stripe errors rather than completely remove them. Moreover, the uncertainty of the fault slips employed for the dislocation model prediction would also contribute to the discrepancies between the GRACE-observed and model-predicted coseismic gravitational changes.

Discussion

The postseismic gravity changes of +0.40 μGal $year^{-1}$, which are predicted by a Maxwell viscosity simulation in the dislocation model for the synthetic test in this study, do not necessarily represent the true postseismic gravity changes following the 2011 Tohoku-Oki earthquake. The Maxwell-body model may not well describe the truth of rheology for the asthenosphere in the Tohoku-Oki earthquake region. The model-predicted linear positive trend of 0.40 μGal $year^{-1}$ for the postseismic gravity changes within two years after the earthquake probably underestimates the postseismic signals, compared with recent studies that demonstrate significant changes and biviscous rheology leading fast relaxation within a few

months to a couple of years (e.g., Han et al. 2014; Hu et al. 2014; Sun et al. 2014; Watanabe et al. 2014). Han et al. (2014) reveal by careful processing to GRACE observations that the postseismic gravity increases by 6 μGal over a 500-km scale within a couple of years after the earthquake, which supports a biviscous relaxation with both transient and steady-state viscosities for the asthenosphere. Thus, the postseismic gravity changes are probably much larger than 0.80 μGal in 2 years and should not be negligible in the GRACE observations. However, it should be noted that the focus of this study is not on postseismic effect but on the retrieval of coseismic changes. The model-predicted postseismic gravity changes are only used to synthesize the seismic-signal-contained observations, for the sake of making the synthetic data as close as possible to the practice (compared with the simple case of synthesizing the observations with coseismic jumps only). In the data processing to retrieve coseismic signals, we remove the postseismic influence (approximately represented by the linear trend after the earthquake) by time series fitting. Therefore, the exact amplitude of postseismic changes would not evidently affect the coseismic signal retrieval. In other words, given much larger amplitude of postseismic gravity changes, the postseismic impact on signal retrieval would still be reduced to a confident level due to the processing of time series fitting. Therefore, the qualitative results and corresponding conclusions from the synthetic test would not change. Moreover, this study places particular emphasis on the coseismic signal detection with GRACE data of short time span after the earthquake (e.g., a few months or even only 1 month of data). The contamination of postseismic effect will not be obvious if data of short time span are employed.

It should be noted that the linear trend after the earthquake to fit the postseismic gravity changes is just a rough approximation within 2 years. A more practical and commonly used representation of the postseismic gravitational changes for GRACE observation is to apply the negative exponential function with a given relaxation time constant (e.g., Han et al. 2008; de Linage et al. 2009; Li et al. 2014) to describe the asthenosphere rheology of earthquake region.

Conclusions

We demonstrate by both synthetic tests and real-data case studies that the coseismic gravitational changes due to the 2011 Tohoku-Oki earthquake are detectable by GRACE with only 1-month data after the earthquake. Model prediction indicates that the negative-positive coseismic gravity changes due to the Tohoku-Oki earthquake range from −11.7 to +5.6 μGal at spatial resolution comparable as that of GRACE, and the corresponding northern gravity gradient changes show a positive-negative-positive pattern with a peak-to-peak range of +2.6 to −2.8 to $+1.2 \times 10^{-13}$ s^{-2}.

The filters applied to GRACE data are critical in retrieving coseismic signals associated with large earthquakes. The results from synthetic tests reveal that the commonly used destriping filter for GRACE data tends to introduce significant amplitude reduction and spatial pattern distortion for coseismic signal extraction. The northern gravity gradient approach with the filter of spatial averaging only (without destriping) is recommended in order to better extract coseismic signals from monthly GRACE solutions. This gradient approach particularly applies for the detection of coseismic signals with limited time span (e.g., a few months after the earthquake) of monthly GRACE solutions and potentially provides a means to constrain fault slip models with large-scale gravitational changes from GRACE observations.

With only 1-month GRACE data of April 2011, we retrieve the coseismic gravitational signals of Tohoku-Oki earthquake using the northern gravity gradient approach. The extracted northern gravity gradient changes show obvious positive-negative-positive spatial pattern that agrees with the model prediction. Even though there are slight amplitude discrepancies between the GRACE observation and model prediction probably due to unfiltered stripe errors as well as fault slip model uncertainties, the detection shows a successful example with only 1-month data and well demonstrates the potential of northern gradient approach to retrieve coseismic signals. Given the postseismic deformation that is particularly evident at large scale (which has been discussed in the above section), the detection of coseismic deformation immediately after the rupture is important. Therefore, the northern gradient approach could be an effective way to process GRACE data and analyze large earthquake deformation.

Competing interests

The authors declare that they have no competing interests.

Authors' contributions

WBS and JL conceived of the idea. WBS designed the plan, and JL completed the computations. WBS and JL discussed the results and drafted the manuscript. Both authors read and approved the final manuscript.

Acknowledgements

We thank the ARIA team at JPL and Caltech for providing the preliminary GPS displacement data (version 0.1). All original GEONET RINEX data are provided to Caltech by the Geospatial Information Authority (GSI) of Japan. We thank CSR for providing the GRACE data. We appreciate the discussion with Drs. Jiancheng Han and Rong Sun about the technical details in plotting the figures. We are grateful to the two anonymous reviewers for their insightful comments, which led to significant improvement of the manuscript. This study is supported by National 973 Project China (grant no. 2013CB733302), NSFC (grant nos. 41174011, 41204017, 41228004, and 41429401), and the Shanghai Postdoctoral Sustentation Fund (grant no. 13R21417900).

Author details

[1]Department of Geophysics, School of Geodesy and Geomatics, Wuhan University, Wuhan 430079, China. [2]Shanghai Astronomical Observatory, Chinese Academy of Sciences, Shanghai 200030, China. [3]State Key Laboratory of Information Engineering in Surveying, Mapping and Remote Sensing, Wuhan University, Wuhan 430079, China.

Received: 3 September 2014 Accepted: 15 January 2015
Published online: 24 February 2015

References

Bassin C, Laske G, Masters GG (2000) The current limits of resolution for surface wave tomography in North America. EOS Trans AGU 81:F897

Cambiotti G, Sabadini R (2012) A source model for the great 2011 Tohoku earthquake (Mw = 9.1) from inversion of GRACE gravity data. Earth Planet Sci Lett 335–336:72–79, doi:10.1016/j.epsl.2012.05.002

Cambiotti G, Sabadini R (2013) Gravitational seismology retrieving centroid-moment-tensor solution of the 2011 Tohoku earthquake. J Geophys Res Solid Earth 118:183–194, doi:10.1029/2012JB009555

Chang ETY, Chao BF (2011) Co-seismic surface deformation of the 2011 off the Pacific coast of Tohoku earthquake: spatio-temporal EOF analysis of GPS data. Earth Planets Space 63:649–654, doi:10.5047/eps.2011.07.002

Chen JL, Wilson CR, Tapley BD, Grand S (2007) GRACE detects coseismic and postseismic deformation from the Sumatra-Andaman earthquake. Geophys Res Lett 34:L13302, doi:10.1029/2007GL030356

Cheng M, Tapley BD (2004) Variations in the Earth's oblateness during the past 28 years. J Geophys Res 109:B09402, doi:10.1029/2004JB003028

Cheng M, Tapley BD, Ries JC (2013) Deceleration in the Earth's oblateness. J Geophys Res 118:740–747, doi:10.1002/jgrb.50058

Dai C, Shum CK, Wang R, Wang L, Guo J, Shang K, Tapley BD (2014) Improved constraints on seismic source parameters of the 2011 Tohoku earthquake from GRACE gravity and gravity gradient changes. Geophys Res Lett 41:1929–1936, doi:10.1002/2013GL059178

de Linage C, Rivera L, Hinderer J, Boy JP, Rogister Y, Lambotte S, Biancale R (2009) Separation of coseismic and postseismic gravity changes for the 2004 Sumatra-Andaman earthquake from 4.6 yr of GRACE observations and modeling of the coseismic change by normal modes summation. Geophys J Int 176:695–714, doi:10.1111/j.1365-246X.2008.04025.x

Duan XJ, Guo JY, Shum CK, van der Wal W (2009) On the postprocessing removal of correlated errors in GRACE temporal gravity field solutions. J Geod 83(11):1095–1106, doi:10.1007/s00190-009-0327-0

Han SC, Shum CK, Bevis M, Ji C, Kuo CY (2006) Crustal dilatation observed by GRACE after the 2004 Sumatra-Andaman earthquake. Science 313:658–662, doi:10.1126/science.1128661

Han SC, Sauber J, Luthcke SB, Ji C, Pollitz FF (2008) Implications of postseismic gravity change following the great 2004 Sumatra–Andaman earthquake from the regional harmonic analysis of GRACE intersatellite tracking data. J Geophys Res 113:B11413, doi:10.1029/2008JB005705

Han SC, Sauber J, Luthcke S (2010) Regional gravity decrease after the 2010 Maule (Chile) earthquake indicates large-scale mass redistribution. Geophys Res Lett 37:L23307, doi:10.1029/2010GL045449

Han SC, Sauber J, Riva R (2011) Contribution of satellite gravimetry to understanding seismic source processes of the 2011 Tohoku-Oki earthquake. Geophys Res Lett 38:L24312, doi:10.1029/2011GL049975

Han SC, Riva R, Sauber J, Okal E (2013) Source parameter inversion for recent great earthquakes from a decade-long observation of global gravity fields. J Geophys Res Solid Earth 118:1240–1267, doi:10.1002/jgrb.50116

Han SC, Sauber J, Pollitz F (2014) Broadscale postseismic gravity change following the 2011 Tohoku-Oki earthquake and implication for deformation by viscoelastic relaxation and afterslip. Geophys Res Lett 41:5797–5805, doi:10.1002/ 2014GL060905

Hayes GP (2011) Rapid source characterization of the 2011 M_w 9.0 off the Pacific coast of Tohoku Earthquake. Earth Planets Space 63:529–534, doi:10.5047/eps.2011.05.012

Heki K, Matsuo K (2010) Coseismic gravity changes of the 2010 earthquake in central Chile from satellite gravimetry. Geophys Res Lett 37:L24306, doi:10.1029/2010GL045335

Hu Y, Bürgmann R, Freymueller JT, Banerjee P, Wang K (2014) Contributions of poroelastic rebound and a weak volcanic arc to the postseismic deformation of the 2011 Tohoku earthquake. Earth Planets Space 66:106, doi:10.1186/1880-5981-66-106

Ito T, Ozawa K, Watanabe T, Sagiya T (2011) Slip distribution of the 2011 off the Pacific coast of Tohoku Earthquake inferred from geodetic data. Earth Planets Space 63:627–630, doi:10.5047/eps.2011.06.023

Kobayashi T, Tobita M, Nishimura T, Suzuki A, Noguchi Y, Yamanaka M (2011) Crustal deformation map for the 2011 off the Pacific coast of Tohoku earthquake detected by InSAR analysis combined with GEONET data. Earth Planets Space 63:621–625, doi:10.5047/eps.2011.06.043

Li J, Shen WB (2011) Investigation of the co-seismic gravity field variations caused by the 2004 Sumatra-Andaman earthquake using monthly GRACE data. J Earth Sci 22:280–291, doi:10.1007/s12583-011-0181-x

Li J, Chen JL, Zhang ZZ (2014) Seismologic applications of GRACE time-variable gravity measurements. Earthq Sci 27(2):229–245, doi:10.1007/s11589-014-0072-1

Matsuo K, Heki K (2011) Coseismic gravity changes of the 2011 Tohoku-Oki earthquake from satellite gravimetry. Geophys Res Lett 38:L00G12, doi:10.1029/2011GL049018

Sato K, Ishii H, Takagi A (1981) Characteristics of crustal tress and crustal movements in the northeastern Japan arc I: based on the computation considering the crustal structure (in Japanese). Zisin (J Seismol Soc Jpn), Ser 2 34:551–564

Sato M, Ishikawa T, Ujihara N, Yoshida S, Fujita M, Mochizuki M, Asada A (2011) Displacement above the hypocenter of the 2011 Tohoku-Oki earthquake. Science 332:1395, doi:10.1126/science.1207401

Shao G, Li X, Ji C, Maeda T (2011) Focal mechanism and slip history of the 2011 Mw 9.1 off the Pacific coast of Tohoku Earthquake constrained with teleseismic body and surface waves. Earth Planets Space 63:559–564, doi:10.5047/eps.2011.06.028

Sleep NH (2012) Constraint on the recurrence of great outer-rise earthquakes from seafloor bathymetry. Earth Planets Space 64:1245–1246, doi:10.5047/eps.2012.07.011

Suito H, Hirahara K (1999) Simulation of postseismic deformations caused by the 1896 Riku-u earthquake, northeast Japan: re-evaluation of the viscosity in the upper mantle. Geophys Res Lett 26:2561–2564

Suito H, Nishimura T, Tobita M, Imakiire T, Ozawa S (2011) Interplate fault slip along the Japan Trench before the occurrence of the 2011 off the Pacific coast of Tohoku Earthquake as inferred from GPS data. Earth Planets Space 63:615–619, doi:10.5047/eps.2011.06.053

Sun W, Okubo S, Fu G, Araya A (2009) General formulations of global co-seismic deformations caused by an arbitrary dislocation in a spherically symmetric earth model—applicable to deformed earth surface and space-fixed point. Geophys J Int 177:817–833, doi:10.1111/j.1365-246X.2009.04113.x

Sun T, Wang K, Iinuma T, Hino R, He J, Fujimoto H, Kido M, Osada Y, Miura S, Ohta Y, Hu Y (2014) Prevalence of viscoelastic relaxation after the 2011 Tohoku-oki earthquake. Nature 514:84–87, doi:10.1038/nature13778

Suzuki K, Hino R, Ito Y, Yamamoto Y, Suzuki S, Fujimoto H, Shinohara M, Abe M, Kawaharada Y, Hasegawa Y, Kaneda Y (2012) Seismicity near the hypocenter of the 2011 off the Pacific coast of Tohoku earthquake deduced by using ocean bottom seismographic data. Earth Planets Space 64:1125–1135, doi:10.5047/eps.2012.04.010

Swenson S, Wahr J (2006) Post-processing removal of correlated errors in GRACE data. Geophys Res Lett 33:L08402, doi:10.1029/2005GL025285

Wang R, Lorenzo-Martín F, Roth F (2006) PSGRN/PSCMP - a new code for calculating co- and post-seismic deformation, geoid and gravity changes based on the viscoelastic-gravitational dislocation theory. Comput Geosci 32:527–541, doi:10.1016/j.cageo.2005.08.006

Wang L, Shum CK, Simons FJ, Tapley BD, Dai C (2012a) Coseismic and postseismic deformation of the 2011 Tohoku-Oki earthquake constrained by GRACE gravimetry. Geophys Res Lett 39:L07301, doi:10.1029/2012GL051104

Wang L, Shum CK, Jekeli C (2012b) Gravitational gradient changes following the 2004 December 26 Sumatra–Andaman earthquake inferred from GRACE. Geophys J Int 191(3):1109–1118, doi:10.1111/j.1365-246X.2012.05674.x

Watanabe S, Sato M, Fujita M, Ishikawa TM, Yokota Y, Ujihara N, Asada A (2014) Evidence of viscoelastic deformation following the 2011 Tohoku-Oki earthquake revealed from seafloor geodetic observation. Geophys Res Lett 41:5789–5796, doi:10.1002/2014GL061134

Wei S, Sladen A, the ARIA group (2011) Updated result, 3/11/2011 (Mw 9.0), Tohoku-Oki, Japan. Available at: http://www.tectonics.caltech.edu/slip_history/2011_taiheiyo-oki/

Zhou X, Sun W, Zhao B, Fu G, Dong J, Nie Z (2012) Geodetic observations detecting coseismic displacements and gravity changes caused by the Mw = 9.0 Tohoku-Oki earthquake. J Geophys Res 117:B05408, doi:10.1029/2011JB008849